

# The Smith Cloud and its dark matter halo: survival of a Galactic disc passage

Matthew Nichols,<sup>1★</sup> Nestor Mirabal,<sup>2†</sup> Oscar Agertz,<sup>3</sup> Felix J. Lockman<sup>4</sup>  
and Joss Bland-Hawthorn<sup>5</sup>

<sup>1</sup>Laboratoire d'Astrophysique, École Polytechnique Fédérale de Lausanne (EPFL), Observatoire de Sauverny, 1290 Versoix, Switzerland

<sup>2</sup>Dpto. de Física Atómica, Molecular y Nuclear, Universidad Complutense de Madrid, Madrid 28040, Spain

<sup>3</sup>Department of Physics, University of Surrey, Guildford, Surrey GU2 7XH, UK

<sup>4</sup>National Radio Astronomy Observatory, PO Box 2, Green Bank, WV 24944, USA

<sup>5</sup>Sydney Institute for Astronomy, School of Physics, The University of Sydney, NSW 2006, Australia

Accepted 2014 May 22. Received 2014 May 21; in original form 2014 April 9

## ABSTRACT

Under conservative assumptions about the Galaxy, the derived velocity of the Smith Cloud indicates that it will have undergone at least one passage of the Galactic disc. Using hydrodynamic simulations, we examine the present-day structure of the Smith Cloud and find that a dark matter supported cloud is able to reproduce the observed present-day neutral hydrogen mass, column density distribution and morphology. In this case, the dark matter halo becomes elongated owing to the tidal interaction with the Galactic disc. Clouds in models neglecting dark matter confinement are destroyed upon disc passage, unless the initial cloud mass is well in excess of what is observed today. We then determine integrated flux upper limits to the gamma-ray emission around such a hypothesized dark matter core in the Smith Cloud. No statistically significant core or extended gamma-ray emission are detected down to a 95 per cent confidence level upper limit of  $1.4 \times 10^{-10}$  ph cm<sup>-2</sup> s<sup>-1</sup> in the 1–300 GeV energy range. For the derived distance of 12.4 kpc, the *Fermi* upper limits set the first tentative constraints on the dark matter cross-sections annihilating into  $\tau^+\tau^-$  and  $b\bar{b}$  for a high-velocity cloud.

**Key words:** ISM: clouds – ISM: individual objects: Smith Cloud – Galaxy: halo – dark matter – gamma-rays: general.

## 1 INTRODUCTION

The mapping of dark matter (DM) substructure around the Galaxy is crucial to understanding how our own Milky Way was assembled over cosmic time. Numerical simulations of the concordant cosmology, dark energy and  $\Lambda$  cold dark matter, predict a multitude of DM subhaloes going down in mass to approximately  $10^{-4} M_\odot$  (e.g. Klypin et al. 1999; Moore et al. 1999; Diemand, Kuhlen & Madau 2007; Springel et al. 2008). On the detectable scale of dwarf galaxies, this discrepancy approaches an order of magnitude between the observed dwarf galaxies and the number of predicted subhaloes (Mateo 1998; Weinberg et al. 2013). Recent discoveries of ultrafaint dwarf galaxies go some way towards filling this gap (e.g. Willman et al. 2005; Belokurov et al. 2007). Unfortunately, due to the minuscule stellar populations, finding ultrafaint dwarfs continues to be challenging and the exact number of them is unknown. The low stellar content of them however, makes them potentially excellent

objects to search for DM annihilation signals (Charbonnier et al. 2011). So far, no significant detections have been made, although upper limits have been placed on the properties of DM (e.g. Abdo et al. 2010; Natarajan et al. 2013; The Fermi-LAT Collaboration et al. 2014).

In addition to dwarf galaxies, the Galactic halo contains a large number of intriguing H I substructures in the form of high-velocity clouds (HVCs; Wakker & van Woerden 1997). The suggestion of DM surrounding a population of these HVCs has been around for over a decade (e.g. Blitz et al. 1999; Quilis & Moore 2001). Subsequent investigation has determined that any such population is likely to be small in comparison to DM-free HVCs, both around our own galaxy (Saul et al. 2012) and also around other galaxies (Chynoweth, Langston & Holley-Bockelmann 2011). Near the disc, some of the HVCs are likely to arise through a galactic fountain, where numerous supernova launch gas from the disc of the Galaxy (Bregman 1980); however, this process is likely to produce small, intermediate velocity clouds over HVCs (Ford, Lockman & McClure-Griffiths 2010). Many HVCs that lie within 50 kpc of the Milky Way likely had their origin in the Magellanic Stream and thus arose from the LMC and SMC (Putman 2004). Extragalactic

\* E-mail: [matthew.nichols@epfl.ch](mailto:matthew.nichols@epfl.ch)

† Ramón y Cajal Fellow.

HVCs are seen at a wide range of projected distances, often exceeding 150 kpc from the nearest galaxy, are likely to be clumps of pristine gas infalling for the first time and possess a phase-space distribution that is incompatible with the expected DM substructure (Chynoweth et al. 2011). Even at low projected distances (<50 kpc) many of the extragalactic HVCs are not associated with regions of star formation suggesting that they too are infalling for the first time (Thilker et al. 2004; Westmeier, Brüns & Kerp 2008). Despite the abundance of other sources for HVCs, explaining why all DM subhaloes that failed to form stars lack any gas is difficult and a small fraction of HVCs may be such objects.

In order to investigate the DM content in H I clouds, we recently searched for gamma-ray emission from DM annihilation at the location of several compact H I clouds in the GALFA-HI Compact Cloud Catalog (Mirabal 2013). However, poorly constrained DM profiles and unknown distances to these objects severely limited our analysis. To advance more thoroughly, we need to examine systems with better distance determinations and are likely to be candidates for DM-embedded HVCs. The best candidate for such a search is the Smith Cloud, a massive H I system near the Galactic disc (Smith 1963). The Smith Cloud is located close by at  $12.4 \pm 1.3$  kpc (Lockman et al. 2008), and of particular appeal is that a DM subhalo seems to be required for the survival of the gas cloud after a passage through the Galactic disc (Nichols & Bland-Hawthorn 2009).

Given its relative proximity, derivable orbit and large mass it appears to qualify as the ideal astrophysical site to test the DM confinement of H I clouds. Here, we search for potential gamma-ray emission from the DM annihilation of weakly interacting particles (WIMPs) around the Smith Cloud. In Section 2, we present arguments in favour of a DM subhalo surrounding the Smith Cloud. Next, we present the *Fermi*-Large Area Telescope (LAT) analysis and derive *Fermi* upper limits to the gamma-ray flux. In Section 5, we turn the results into limits on annihilation cross-sections. Finally, we summarize our results and present our conclusions.

## 2 THE SMITH CLOUD AND A DM HALO

Most HVCs do not require DM to explain their survivability and formation, being able to form through galactic fountains, tidal stripping of gas or condensation of primordial gas. We argue that none of these processes are likely to have created the Smith Cloud, and that a gas cloud encapsulated by DM provides the best model.

The Smith Cloud is an extraordinary gas structure with a cometary tail being accreted on to the Galaxy (Lockman et al. 2008; Nichols & Bland-Hawthorn 2009). Unusually for an HVC, the distance to the Smith Cloud is relatively well known (to within 20 per cent). Based on stellar bracketing (Wakker et al. 2008), interaction of stripped material with disc gas (Lockman et al. 2008) and the flux of H $\alpha$  reflected from the Galactic disc (Bland-Hawthorn et al. 1998; Putman et al. 2003), the distance to the Smith Cloud is known to be  $12.4 \pm 1.3$  kpc (Lockman et al. 2008).

Here, we use H I 21 cm data from a preliminary reduction of a new survey of the Smith Cloud with the 100 meter Green Bank Telescope (GBT) of the National Radio Astronomy Observatory.<sup>1</sup> The new survey covers more than twice the area of the Lockman et al. (2008) survey and uses a different spectrometer that provides four times the velocity resolution ( $0.32 \text{ km s}^{-1}$ )

over a 1.6 times greater Local Standard of Rest (LSR) velocity range,  $-400$  to  $+400 \text{ km s}^{-1}$  LSR. The preliminary reduction of the new survey data has a median noise level of 65 mK, a factor 1.5 times more sensitive than the previous survey, and the observing and reduction techniques produce maps at the full 9.1 arcmin resolution of the GBT. The new survey is also corrected for residual stray radiation (Boothroyd et al. 2011) improving the dynamic range at low velocities. The new data show that the Smith Cloud is considerably more extended than previously thought, with a diffuse tail to at least  $l, b = 50, -25$  and components that appear to have been detached from the main structure (e.g. at  $38, -18$  and  $40, -22$ ). The observations are nearing completion and the full data set will be published separately.

The existence of a velocity gradient across the cloud and knowledge of its position allows a determination of the true 3D velocity (and consequent orbit) if the Smith Cloud is travelling along the plane of the sky. The orbit is calculated using the potential from Wolfire (1995) as detailed in Lockman et al. (2008). Using the orbital determination of Lockman et al. (2008), the cloud will have passed through the disc approximately 70 Myr ago at a radius of 13 kpc. Such an orbit assumes that the velocity gradient is towards the lower end, that drag is minimal along the Smith Cloud's orbit, and the current distance estimate is correct. We have examined the effects of changing the velocity gradient, distance and introducing drag with coefficients of drag up to  $C_D = 5$ . Even with the most generous assumptions of drag, distance and velocity gradient, the total velocity of the Smith Cloud is restricted by observations to  $\sim 300 \text{ km s}^{-1}$  and so cannot have fallen in from infinity. Furthermore, in all but the most extreme cases, the Smith Clouds orbit will pass through the disc at a radius of approximately 13 kpc, and hence the cloud must have passed through the disc or been created in the past  $\sim 70$  Myr.

### 2.1 Galactic fountains

Compared to most of the H I clouds that surround the Milky Way, the Smith Cloud is exceptionally massive, with a gas mass exceeding  $2 \times 10^6 M_\odot$ . Correspondingly, the energy contained in the Smith Cloud is also extremely large compared to the gas at any potential launching point inside the Galactic disc ( $\sim 1.0 \times 10^{54}$  erg). This tremendous energy budget would require of the order of 1000 supernova in order to produce sufficient energy to dislodge the Smith Cloud inside a galactic fountain. Such a process would also have to take place at a radius  $\sim 13$  kpc (the distance where the Smith Cloud's orbit intersects the disc  $\sim 70$  Myr ago) in order to be produced (such a simple calculation is in line with a linear scaling of galactic fountain hydrodynamic simulations by de Gouveia Dal Pino et al. 2009). The requirements of a massive cluster at a large radius hence make it extremely unlikely that the Smith Cloud was formed through any galactic fountain.

That the Smith Cloud would be exceptionally rare if it was a product of the galactic fountain is further supported by the fact that the largest observed H I cloud elevated by a supershell is only  $3 \times 10^4 M_\odot$  and, like most gas clouds associated with the galactic fountain, has a low peculiar velocity relative to the disc (Pidopryhora, Lockman & Shields 2007).

If it did not arise directly from the disc, it is still possible to have avoided a disc passage if it had undergone a tidal interaction in the recent past. However, there is no obvious candidate to have provided such a massive cloud and given the paucity of dwarf galaxies that contain gas (Grcevich & Putman 2009), the detection of a suitable host that until recently held gas would raise further questions.

<sup>1</sup> The National Radio Astronomy Observatory is a facility of the National Science Foundation operated by Associated Universities, Inc.

## 2.2 Passage through the disc

Without arising from the disc and a tidal event being unlikely, the original origin of the Smith Cloud is likely to be from extragalactic infalling gas. Such HVCs are potentially able to survive to near the disc without any DM through ablative shielding (Plöckinger & Hensler 2012; Putman, Peek & Joung 2012). In particular, Plöckinger & Hensler (2012) suggest that DM will suppress the characteristic substructure present within HVCs as they approach the disc. However, little work has been done on the passage of HVCs through the disc, potentially the biggest impediment to the survival of the Smith Cloud.

We note that the current cloud total velocity, relative to the expected Milky Way virial velocity  $|V_{\text{tot}}/V_{\text{vir}}| \sim 2$ , is compatible with phase-space data of substructure at  $r \sim 10$  kpc in simulated high-resolution DM haloes of Milky Way mass (Boylan-Kolchin et al. 2012).

At 13 kpc, the surface density of the disc is approximately  $3 \times 10^{20} \text{ cm}^{-2}$  (Kalberla & Dedes 2008) and is increased by a factor of 3 due to the oblique angle at which the Smith Cloud passes through the disc. At such high-column-densities, gas clouds passing through the disc are likely to be heavily disrupted. Simple toy models presented in Nichols & Bland-Hawthorn (2009) suggest that this disc passage and ram pressure stripping throughout the orbit will require a DM halo to survive to the present day.

We supplement the toy model argument presented previously, which suggested a DM halo of  $M_{\text{tid}} \sim 2 \times 10^8 - 1 \times 10^9 M_{\odot}$ , with numerical simulations of a cloud passing through a disc with and without a supporting DM halo.

## 2.3 Numerical simulations

In an attempt to replicate the observed mass, morphology and H I distribution of the Smith Cloud today, shown in Fig. 1, we

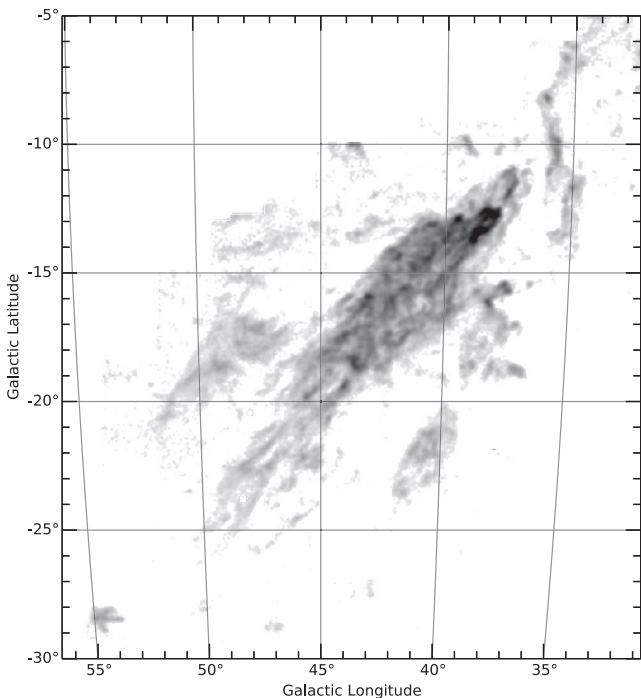


**Figure 1.** GBT H I image of the Smith Cloud integrating over all  $V_{\text{GSR}} > 220 \text{ km s}^{-1}$ . The grey-scale is proportional to the square root of the H I column density to reveal the extended cometary morphology.

use the adaptive mesh refinement (AMR) code RAMSES (Teyssier 2002).

Using RAMSES, we simulate the disc passage of both a DM-enclosed H I cloud and a DM-free cloud, along the Smith Cloud’s expected orbital path from peak height above the disc 204 Myr ago and compare that to new H I observations. We include a realistic progenitor to the Smith Cloud and a realistic model of the Milky Way which includes live stellar and gaseous discs and DM halo. We evolve the coupled  $N$ -body and hydrodynamical system while accounting for metal dependent radiative cooling and UV background heating as per Agertz et al. (2013) at a maximum resolution of  $\Delta x \sim 18 \text{ pc}$ .

The Smith Cloud progenitor is modelled over a range of densities,  $n = 0.1 - 0.5 \text{ cm}^{-3}$  in  $0.1 \text{ cm}^{-3}$  steps, with a constant size,  $r = 0.5 \text{ kpc}$ , in order to explore the potential parameter space of the Smith Cloud. Such a range ( $M_{\text{H I, initial}} = 1.3 - 7.8 \times 10^6 M_{\odot}$ ) includes clouds approximately half the mass of the Smith Cloud and to clouds approximately three times bigger than the Smith Cloud today, but in line with massive clouds in nearby systems (e.g. Chynoweth et al. 2008) as well as allowing a large degree of mass-loss to the present day. In order to model the survival with and without a DM halo, we consider both a pressure supported cloud and one which is embedded within a Navarro–Frenk–White (NFW) DM halo of virial mass  $M_{\text{NFW}} = 3 \times 10^8 M_{\odot}$  and concentration  $c = 30$ .

The model Galaxy is considered to consist of a Galactic disc of total mass  $M_{\text{disc}} = 4.3 \times 10^{10} M_{\odot}$ , where the gaseous disc accounts for  $8.6 \times 10^9 M_{\odot}$  of the baryons. The disc has a scale radius of  $r_{\text{disc}} = 3.4 \text{ kpc}$  and an exponential scaleheight  $h = 0.1 r_{\text{disc}}$ . These discs are embedded inside a hot gaseous halo with density  $n = 10^{-3} \text{ cm}^{-3}$ , a reasonable density out to  $r \sim 10 - 30 \text{ kpc}$  (Gatto et al. 2013), along with an  $M_{\text{vir}} = 10^{12} M_{\odot}$  NFW DM halo with concentration  $c = 10$ . Note that the adopted gaseous halo density, out to the initial simulation cloud altitude ( $z \sim 20 \text{ kpc}$ ) 204 Myr ago, is a *conservative* choice, as the observed circumdisc medium likely is denser; Savage & Wakker (2009) using corrected fits to the data of Gaensler et al. (2008) found that a warm gaseous disc of the form  $n(z) = n_0 \exp(-z/H)$ , where  $n_0 = 0.016 \text{ cm}^{-3}$  and  $H = 1.4 \text{ kpc}$ , is consistent with the Milky Way.

In Fig. 2, we display the initial and the H I mass that would be observed today of the simulated clouds. DM-free clouds with densities below  $n = 0.4 \text{ cm}^{-3}$ , initial masses below  $5 \times 10^6 M_{\odot}$ , are entirely destroyed by their passage through the hot halo and Galactic disc. Clouds with densities above this survive the passage, with nearly all of their mass intact. In contrast to the baryon-only clouds, the DM-supported clouds at all masses manage to pass through the disc of the Galaxy with minimal mass-loss, or at higher ends, a small gain due to gas accreted from the disc.

The morphological features of the H I are also examined. In Fig. 3, we show the observed H I density today (rescaled to maximum density in each case), for both DM-free clouds (top row) and DM-encapsulated clouds (bottom row). We display only the middle three densities as these adequately show the evolution of the cloud with mass.

At the lowest density considered,  $n = 0.1 \text{ cm}^{-3}$  (not shown), the DM-free cloud is destroyed, while in the DM case, the H I is completely separated from the DM halo and lacks the dense features reminiscent of the Smith Cloud. Such a stripped cloud will then likely be destroyed at the next disc passage as a DM-free cloud.

At  $n = 0.2 \text{ cm}^{-3}$ , the DM-free cloud is again destroyed, with no observable remnant surviving. In contrast, the DM-supported cloud survives, with a dense core and recently shed cloudlets,

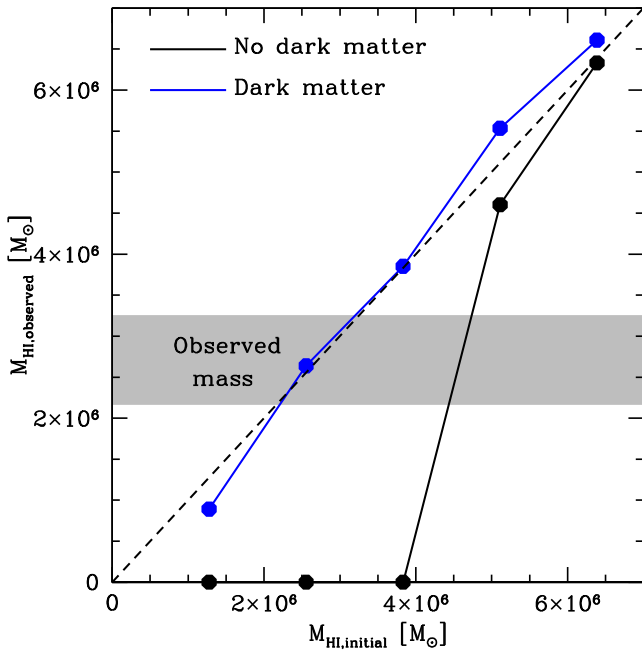


**Figure 2.** Initial H I mass versus the mass that would be observed today. DM-free models are shown as black points (lower line) and DM models in blue (upper line). The dashed line shows a 1:1 correspondence, points below this represent clouds which have lost mass and points above will have accreted mass over the simulation. The observed mass of the Smith Cloud is shown as a grey bar as calculated from the H I distribution of the Smith Cloud.

producing an extended fragmented structure reminiscent of the observed cloud.

At  $n = 0.3 \text{ cm}^{-3}$ , the DM-free cloud retains little mass, but has an observable structure. However, this cloud retains only a smooth, low-column-density structure. The DM-encapsulated cloud meanwhile retains the dense clumps but, in addition to being more massive than the observed cloud, suffers little fragmentation, with long tendrils that would be readily observable. In both cases the low-density gas that is present displays a hatched pattern, a graphical artefact, arising from the conversion between coarse low-density AMR grids and the higher density grids used for plotting. Such graphical artefacts only arise at column densities well below the vast majority of the Smith Cloud and hence can be safely ignored when considering the morphology.

At  $n = 0.4 \text{ cm}^{-3}$ , the DM-free cloud is massive enough to survive its passage through the disc of the Galaxy, and begins to fragment. While portions of it follow the orbital path, a large portion of it has been stripped, and suffering from drag extends the cloud to higher Galactic longitudes at approximately constant latitude. Such a structure is not seen in the Smith Cloud today, and once again contains too much mass. The DM cloud again displays the tendrils with little fragmentation compared to the central clump, but again contains too much mass to be equivalent today.

At  $n = 0.5 \text{ cm}^{-3}$  (not shown), the clouds are almost identical. Both display the tendrils associated with high-mass clouds, as well as a dense core. In addition to the morphological differences, both clouds contain too much mass to be representative of the Smith Cloud today.

Due to the added gravitational attraction of the baryonic disc, the DM core of the HVC becomes significantly elongated. We show this distortion in Fig. 4, comparing the initial conditions with the final

result for a DM-encapsulated cloud with a density of  $n = 0.2 \text{ cm}^{-3}$ . The DM subhalo finishes with a flattening of  $\sim 1/2$  due to tidal forces of the disc. Such a transformation from a spherical halo to a roughly prolate spheroid differs from the expected result from DM only simulations, where tidal forces tend to make a subhalo more spherical (Moore et al. 2004).

The column-density-weighted probability density function is shown in Fig. 5 for both the best-fitting, DM-embedded model (left-hand panel;  $n = 0.2 \text{ cm}^{-3}$ ,  $M_{\text{HI,obs}} = 2.6 \times 10^6 M_{\odot}$ ) and the high-density model (right-hand panel;  $n = 0.5 \text{ cm}^{-3}$ ,  $M_{\text{HI,obs}} = 6.4 \times 10^6 M_{\odot}$ ) both with and without DM. The low-density, DM-embedded model follows the observed distribution remarkably well, replicating the general shape and drop off at column densities exceeding  $1 \times 10^{20} \text{ cm}^{-2}$ , with only occasional clumps above this limit. Compared to this, both high-density models do not begin to drop off until  $\sim 3 \times 10^{20} \text{ cm}^{-2}$ , and retain clumps of gas above this limit. Such clumps approach or exceed the lower limit of star formation free regions in dwarf galaxies (Ekta, Chengalur & Pustilnik 2008) suggesting that such a cloud would begin forming stars regardless of the DM content.

Shown in Fig. 6, the best-fitting model also displays a velocity gradient reminiscent of the observed cloud. The velocity gradient is shown in terms of  $V_{\text{GSR}} = V_{\text{LSR}} + 220 \sin(l) \cos(b) \text{ km s}^{-1}$ , with the simulated cloud having a velocity gradient  $\sim 7 \text{ km s}^{-1} \text{ deg}^{-1}$ . This is in contrast to the observed Smith Cloud which possess a velocity gradient  $\sim 4 \text{ km s}^{-1} \text{ deg}^{-1}$  (see fig. 3 Lockman et al. 2008). However, due to the large degree of variation in both figures, such a discrepancy is not significant.

## 2.4 DM properties

Given the above problems for a DM-free Smith Cloud, the assumption of an encapsulating DM halo remains a viable hypothesis. A simple range on the mass of the DM halo can be calculated by examining two boundary conditions. If the halo is not massive enough it will face the same problems as a DM-free cloud and will quickly smooth out after passing through the disc. If it is too massive, the potential well will have enabled star formation to take place inside the core of the Smith Cloud, something for which there is no evidence.

Analytic limits are explored in Nichols & Bland-Hawthorn (2009) which, for an NFW profile, gives limits corresponding to a dwarf galaxy sized DM halo  $M_{\text{vir}} = 10^9 M_{\odot}$ , although this may vary by at least a factor of 3. Such a halo corresponds to  $r_s \sim 1\text{--}1.8 \text{ kpc}$  and  $\rho_s \sim 6 \times 10^6\text{--}2 \times 10^7 M_{\odot} \text{ kpc}^{-3}$ .

## 3 Fermi-LAT OBSERVATIONS AND ANALYSIS

To search for gamma-ray emission associated with the Smith Cloud, we use *Fermi*-LAT observations carried out from 2008 August 4 to 2013 June 11 (4.85 years of data), corresponding to the interval from 239557417 to 392621346 in Mission Elapsed Time. The analysis is performed using the v9r27p1 *Fermi* Science Tools together with the standard P7SOURCE\_V6 instrument response function. In order to minimize contamination by the Earth's limb, we exclude events with zenith angles  $> 100^\circ$ . We also filter the data using the `gtmktime` filter expression recommended by the LAT team, namely `'(DATA_QUAL==1) && (LAT_CONFIG==1) && ABS(ROCK_ANGLE)<52'`. Fig. 7 shows photon count maps for 100 MeV–1 GeV and 1–300 GeV with contours of integrated H I emission from the Smith Cloud superimposed in green. With the

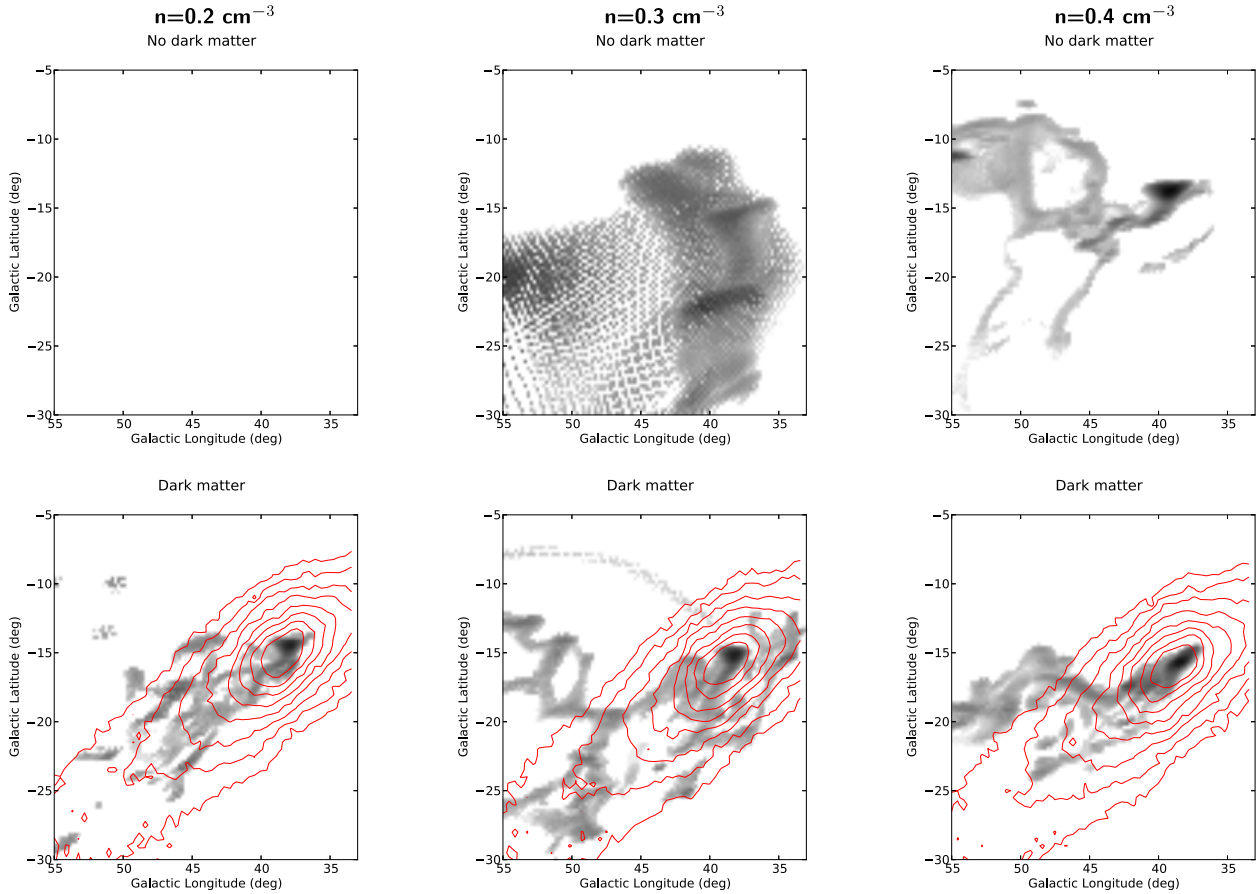


**Figure 3.** Simulated H I intensity for a HVC that has passed through the Galactic disc, without DM (top row) or encapsulated by a DM halo (bottom row). The columns correspond to the initial density of the H I cloud, from left to right,  $n = 0.2 \text{ cm}^{-3}$ ,  $0.3 \text{ cm}^{-3}$  and  $0.4 \text{ cm}^{-3}$ . Each plot is scaled to the simulation maximum H I column density. In the DM present cases, the contours, shown in (red) solid lines, represent the average line of sight DM density between  $10^8$  and  $10^6 M_{\odot} \text{ kpc}^{-3}$  in 0.25 dex steps. The hatched pattern displayed in the low-density gas present in the  $n = 0.3 \text{ cm}^{-3}$  figures is a graphical artefact, arising from the conversion between coarse low-density AMR grids and the higher density grids used for plotting. This hatching only arises at column densities well below the vast majority of the Smith Cloud and hence can be safely ignored when considering the morphology.

current *Fermi* data, we do not see any obvious morphological correspondence between the gamma-ray emission and the observed H I cometary morphology.

An interesting possibility is that there may be additional spatially extended emission if the cloud was removed from the DM due to the shock of passing through the disc. In order to constrain such scenario, we sum gamma-ray counts over the entire orbit of the Smith Cloud. We consider photons within  $\pm 1^\circ$  along the orbit, roughly corresponding to the 95 percent containment angle of the *Fermi* LAT for energies above 10 GeV. Point and extended 2FGL sources listed in Nolan et al. (2012) are masked since they can contaminate the actual cloud contribution. The counts are then compared with the observed counts in the anti-orbit of the cloud, corresponding to the same Galactic longitude but with opposite sign in Galactic latitude. Compared to its anti-orbit, we find no statistically significant gamma-ray excess in the orbit for energies above 1 GeV. The presence of gamma-ray point sources present along the vicinity of the orbit masks important portions of the trajectory, but at present this seems the only reasonable procedure.

Given the absence of extended gamma-ray emission, events are only extracted within a  $10^\circ$  radius centred on the current position of the hypothesized DM subhalo core at  $(\ell, b) = (38.5, -13.4)$ . This final step, in practice, assumes that the subhalo has retained its integrity during the orbit, which the simulations suggest is likely.

The data set is analysed using the binned likelihood method, implemented as the *gtlike* tool in the standard *Fermi* Science Tools.<sup>2</sup> At the position of the Smith Cloud, we create a count map within our region of interest with *gtbin*. We then generate a binned exposure map with *gtexpcube2*, and a model source/diffuse count map with *gtsrcMaps*. In order to place an upper limit for the integrated photon flux, we take advantage of the implementation of *LATAnalysisScripts*.<sup>3</sup> Upper limits are computed with *calcUpper* assuming a power-law spectrum with photon index  $\Gamma = 2$ . The 95 percent confidence upper limit in the 1–300 GeV energy range is  $1.4 \times 10^{-10} \text{ ph cm}^{-2} \text{ s}^{-1}$ .

#### 4 BOUNDS ON DM CROSS-SECTIONS

Our next task is to translate the derived *Fermi* upper limits into actual constraints on annihilation cross-sections. In order to do so,

<sup>2</sup> [http://fermi.gsfc.nasa.gov/ssc/data/analysis/scitools/binned\\_likelihood\\_tutorial.html](http://fermi.gsfc.nasa.gov/ssc/data/analysis/scitools/binned_likelihood_tutorial.html)

<sup>3</sup> <http://fermi.gsfc.nasa.gov/ssc/data/analysis/scitools/LATAnalysisScripts.html>

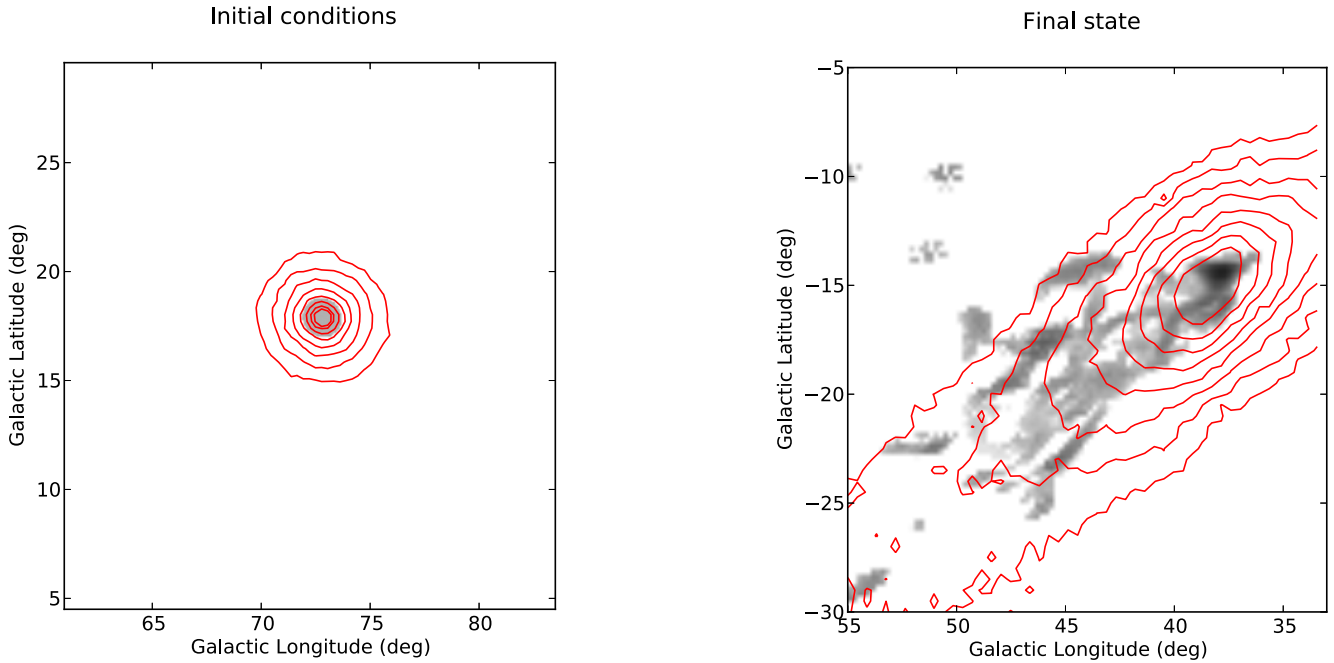


**Figure 4.** Initial and final state (for the best-fitting  $n = 0.2 \text{ cm}^{-3}$  model) for the simulated cloud, with DM contours as in Fig. 3. The grey-scale represents the relative column density across both clouds and is not equivalent between the figures. The initial conditions are the same for all models with only the gas density changed as required. In addition to the gas being disturbed by ram pressure and passage through the disc, the DM is also disturbed due to the gravitational forces on the disc.

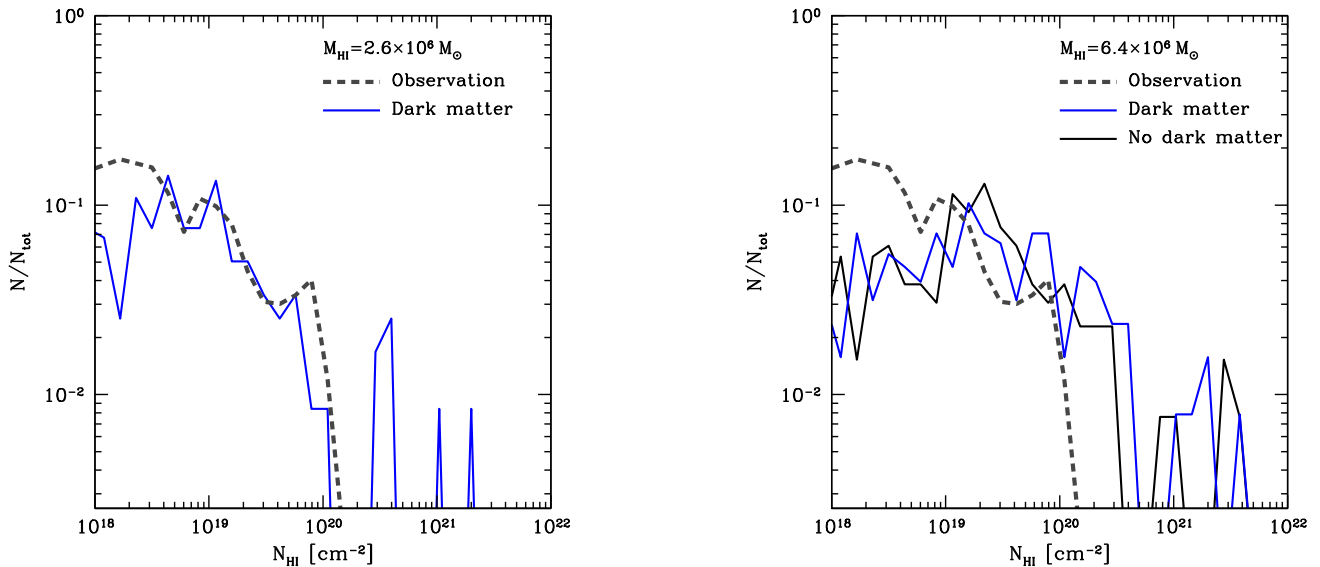


**Figure 5.** Mass-weighted probability function of H column density within the modelled clouds. The left-hand panel shows an  $n = 0.2 \text{ cm}^{-3}$ ,  $M_{\text{H I}} = 2.6 \times 10^6 M_{\odot}$ , DM-embedded cloud in blue. The right-hand panel shows  $n = 0.5 \text{ cm}^{-3}$ ,  $M_{\text{H I}} = 6.4 \times 10^6 M_{\odot}$ , DM free in black and DM-embedded clouds in blue. In both panels, the observed distribution of the Smith Cloud is shown as a grey dashed line.

we use the predicted gamma-ray flux from DM annihilation (Baltz et al. 2008) that can be written as

$$\Phi_{\gamma}(E_{\gamma}, \Delta\Omega) = \Phi^{\text{pp}}(E_{\gamma}) \times J(\Delta\Omega), \quad (1)$$

where  $\Phi^{\text{pp}}(E_{\gamma})$  is the ‘particle physics factor’ that measures the number of gamma-ray photons per DM annihilation. The quantity  $J$  is the ‘astrophysical factor’ which depends on the integral of the

DM distribution  $\rho_{\text{DM}}$  over the line of sight  $l$ . According to this model,

$$J = \int_{\Delta\Omega} \int \rho_{\text{DM}}^2(l, \Omega) dl d\Omega. \quad (2)$$

Here, the solid angle  $\Delta\Omega$  as a function of the integration angle  $\alpha_{\text{int}}$  is defined as

$$\Delta\Omega = 2\pi(1 - \cos(\alpha_{\text{int}})). \quad (3)$$

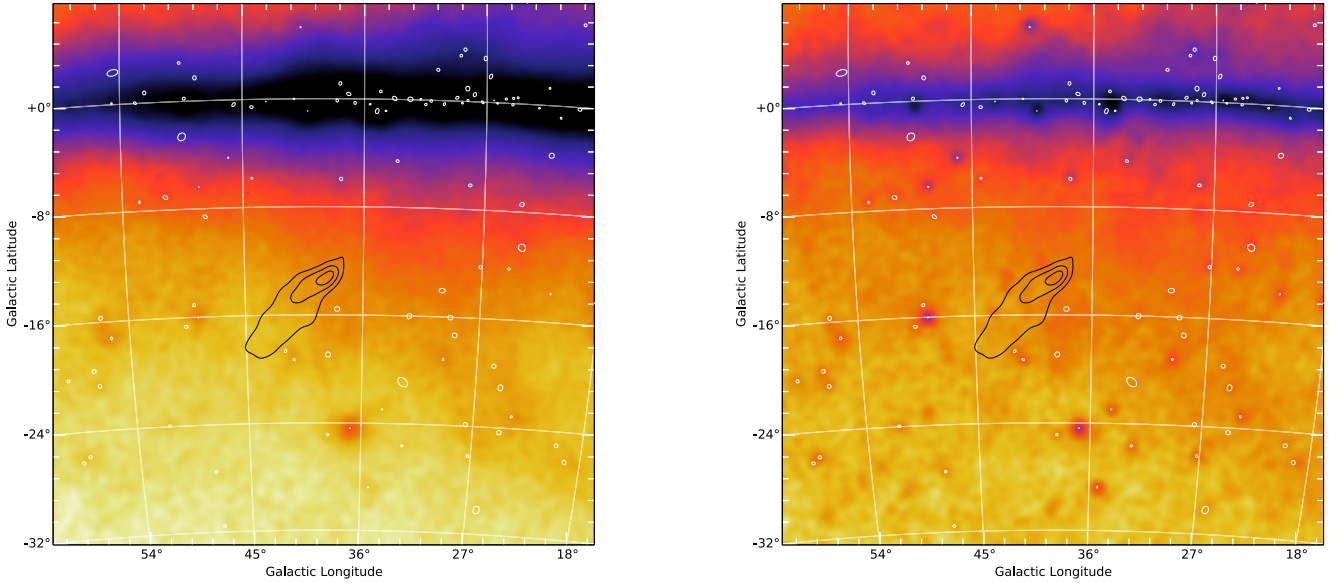


**Figure 6.** H I  $V_{\text{GSR}}$  for a  $2.6 \times 10^6 M_{\odot}$  HVC that has passed through the Galactic disc, encapsulated by DM halo. This model was the best fit of the simulation runs, showing morphological structure reminiscent of the Smith Cloud. The model cloud encapsulated by DM has a velocity gradient as observed in the present-day Smith Cloud (Lockman et al. 2008), although the model gradient is slightly steeper.

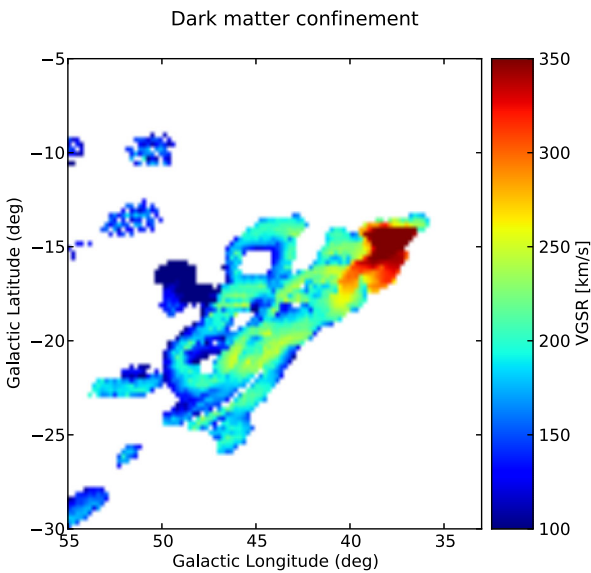


**Figure 7.** Smoothed *Fermi*-LAT count maps of a  $40^{\circ} \times 40^{\circ}$  region around the simulated Smith Cloud for 100 MeV–1 GeV (left) and 1–300 GeV (right), respectively. H I contours for the Smith Cloud are overlaid in green. As the DM halo closely follows the H I distribution, this is also approximately the expected DM location. The white symbols pinpoint 95 percent confidence ellipses of 2FGL point sources (Nolan et al. 2012).

As emphasized previously, since we do not know actually know where in the orbit of Smith the DM subhalo is located, we are making the simplified assumption – supported by simulations – that it is still mostly intact at the head of the cometary structure after its passage of the Galactic disc. We can then estimate  $J$  assuming the values for the DM distribution from Section 2. All calculations of  $J$  presented therein have been obtained with the `CLUMPY` package (Charbonnier, Combet & Maurin 2012). For the DM

subhalo, we consider a canonical NFW profile (Navarro, Frenk & White 1996),

$$\rho_{\text{NFW}}(r) = \rho_s \left( \frac{r}{r_s} \right)^{-1} \left[ 1 + \left( \frac{r}{r_s} \right) \right]^{-2}. \quad (4)$$

where  $\rho_s$  is the scale density, and  $r_s$  is the scale radius. For the actual computation, we adopt  $\rho_s = 1.5 \times 10^7 M_{\odot} \text{ kpc}^{-3}$  and  $r_s = 1.04 \text{ kpc}$  from Nichols & Bland-Hawthorn (2009), a value approximately equal to the DM halo in numerical simulations. Integrating with  $\alpha_{\text{int}} = 0.1$  (used throughout the text) which is compatible with the *Fermi*-LAT PSF at energies  $> 1 \text{ GeV}$ , we find  $\log_{10} J_{\text{NFW}} = 18.44 \text{ GeV}^2 \text{ cm}^{-5}$ .

To allow for a different spatial model, we can also calculate the DM distribution with an Einasto profile (Einasto 1965; Springel et al. 2008) of the form,

$$\rho_{\text{E}}(r) = \rho_{-2} \exp \left\{ -\frac{2}{\alpha} \left[ \left( \frac{r}{r_{-2}} \right)^{\alpha} - 1 \right] \right\}, \quad (5)$$

where  $r_{-2}$  marks the radius where the slope of the profile equals the isothermal value  $\gamma = 2$ , and  $\alpha \sim 0.18$  is the Einasto parameter. We assume the scalings provided by Navarro et al. (2010) so that  $r_{-2} = r_d$ , and  $\rho_s = 4\rho_{-2}$ , respectively. This increases the value of the astrophysical value slightly to  $\log_{10} J_{\text{E}} = 18.52 \text{ GeV}^2 \text{ cm}^{-5}$ .

Referring back to Baltz et al. (2008), we can write the particle physics term  $\Phi^{\text{pp}}(E_{\gamma})$  as

$$\Phi^{\text{pp}}(E_{\gamma}) \equiv \frac{d\Phi_{\gamma}}{dE_{\gamma}} = \frac{1}{4\pi} \frac{\langle \sigma v \rangle}{2m_{\chi}^2} \times \sum_f \frac{dN_{\gamma}}{dE_{\gamma}} B_f, \quad (6)$$

where  $\langle \sigma v \rangle_{\chi}$  is the averaged annihilation cross-section times the relative velocity,  $m_{\chi}$  is the DM particle mass,  $dN_{\gamma}/dE_{\gamma}$  is the photon yield per annihilation final state  $f$ , and  $B_f$  is the branching ratio. For our calculations of  $dN_{\gamma}/dE_{\gamma}$ , we use the analytical fits to `PYTHIA` simulation spectra provided in Fornengo, Pieri & Scopel (2004). We only consider DM annihilating into  $\tau$ -lepton pair ( $\tau^+ \tau^-$ ) and

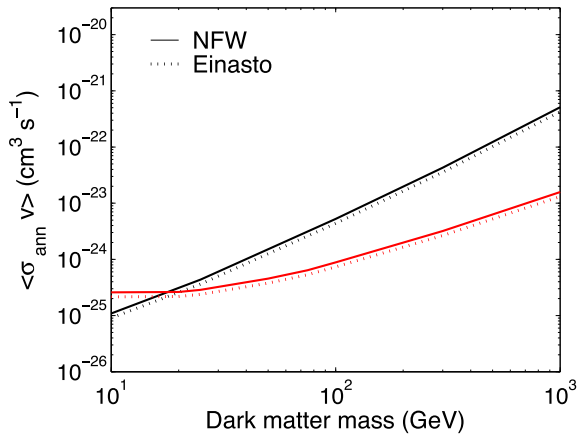


**Figure 8.** Derived upper limits for  $\langle \sigma v \rangle_{\chi}$  versus DM mass for both the NFW and Einasto profiles.  $\tau^+\tau^-$  (black) and  $b\bar{b}$  (red) channels are shown.

bottom quark ( $b\bar{b}$ ) final states. Fig. 8 shows the cross-section upper limits as a function of DM mass for both channels.

## 5 DISCUSSION AND CONCLUSIONS

We have undertaken analytic calculations and numeric simulations to investigate whether the Smith Cloud is encapsulated within a DM halo. In the absence of DM, only the most dense and correspondingly massive clouds survive the passage through the disc of the Galaxy. Such massive objects show column densities much higher than the Smith Cloud is observed to have, and morphologically consist of a dense core with connected tendrils of gas. With a DM halo, an HVC is able to survive the passage through substantially intact. At low densities,  $n \sim 0.2 \text{ cm}^{-3}$ , the resulting cloud contains a column density similar to that of the Smith Cloud and a similar morphological structure to the Smith Cloud of fragmented clumps unattached to the main structure but following the orbit. Such simulations suggest that the idea of the Smith Cloud being encapsulated by a DM halo remains plausible, in particular for this orbit, morphology and  $N_{\text{H I}}$  distribution.

For more massive clouds, the inner densities are approaching that of star-forming regions in metal-poor dwarf galaxies (Ekta et al. 2008). The spatial segregation of gas-free dSphs and dIrrs, where the former is mostly found close to the main galaxy, in the Milky Way and Andromeda is evidence for efficient gas stripping closer to the halo centres (Grevech & Putman 2009). Any star formation would lead to supernova feedback greatly assisting the stripping of gas from the HVC (Gatto et al. 2013), regardless of the presence of DM. In light of Gatto et al. (2013), the absence of stellar feedback in the Smith Cloud makes the fact that we see such a gas-rich structure, which possibly is an ‘unformed’ dwarf galaxy, less of a timing problem, as the compact gas cloud may survive many disc crossings without being completely destroyed via ram pressure/tidal stripping. To fully understand the plausibility of relating an object like the Smith Cloud to non-star-forming substructure, a fully cosmological context is necessary. The initial conditions here are reminiscent of an isolated gas cloud, but such conditions are likely to be unrealistic for the Smith Cloud as tracing its predicted orbit back further in time indicates that it will have crossed the disc multiple times. Such a simplified set of initial conditions is unlikely to impact the major results however. While no simulation traced the evolution back through a full orbit, simulations were continued until after the next disc crossing. In this case, despite the DM halo being flattened by

the disc, the Smith Cloud still survives the disc passage with most of its mass intact.

If encapsulated by DM, the Smith Cloud therefore inhabits a narrow region between being too light to survive ram pressure removing it from the host DM subhalo and being too massive with resulting star formation greatly assisting this stripping. Using the simplistic range from Nichols & Bland-Hawthorn (2009) suggests that a virial mass range of  $\sim 10^8$ – $10^9$  could host the Smith Cloud without being too small to protect the enclosed gas or too large with resulting star formation. A Milky Way-sized galaxy could expect  $\sim 60$  haloes within this mass range (Diemand et al. 2007). HVCs like the Smith Cloud are, however, rare suggesting that either the lower mass end is unrealistically low, or something removes most of the gas from the majority of these haloes.

We neglect the magnetic field that has recently been observed inside the Smith Cloud (Hill et al. 2013). The magnetic field may help stabilize a DM-free cloud minimizing the loss of gas from the cloud (Konz, Brüns & Birk 2002). Whether such a field would be sufficient to protect the Smith Cloud is unknown and should be investigated further.

We report photon flux upper limits for the gamma-ray emission at the current position of the Smith Cloud using 4.85 years of accumulated *Fermi*-LAT data to investigate the properties of such a DM halo. We exclude WIMPs annihilating into  $\tau^+\tau^-$  and  $b\bar{b}$  final states down to  $\langle \sigma v \rangle_{\chi} \sim 3 \times 10^{-25} \text{ cm}^3 \text{ s}^{-1}$  for masses around 10 GeV. The obvious caveat is that DM might have been shed during the history of the cloud; however, the simulations have the DM retain the cloud core up to its present-day location with only minor elongation. To investigate this case, we compare the counts from the projected orbit and anti-orbit. We find no evidence for excess gamma-ray emission along the predicted trajectory of the cloud system. In addition, there is no morphological gamma-ray structures overlapping the cometary structure reported in H I. Despite this failed effort, gamma-ray observations still offers one of the few available opportunities to diagnose the DM content of gaseous clouds. Upcoming experiments such as the Cherenkov Telescope Array will be able to achieve improved angular resolution and sensitivity around the Smith Cloud for energies above 100 GeV (CTA Consortium 2013; Doro et al. 2013). The velocity-averaged annihilation cross-section upper bounds obtained around the Smith Cloud are compatible with limits from other searches reported in the dwarf galaxies (Abdo et al. 2010) and galaxy clusters (Ackermann et al. 2010).

After submission, we became aware of a similar investigation by Drlica-Wagner et al. (2014), who also searched for gamma-ray emission resulting from DM self-annihilation in the Smith Cloud. Using an extended source search around the halo posited in Nichols & Bland-Hawthorn (2009), they achieve limits an order of magnitude lower on the cross-section upper bounds than that presented here. The caveats mentioned on the existence of the DM subhalo above will also apply to their results.

Our results rest upon the assumption that there is indeed a DM subhalo seeding the Smith Cloud. To this extent we undertook simulations demonstrating that such an assumption is plausible given the disc passage the Smith Cloud is likely to have undertaken. As well as demonstrating that the Smith Cloud’s structure can be reproduced through a DM-embedded HVC, such a result suggests that clouds with DM that have passed a disc may take on the comet like morphology observed in expected in DM-free HVCs which have not yet crossed the disc (e.g. Putman, Saul & Mets 2011; Plöckinger & Hensler 2012). Whether the Smith Cloud does in fact contain DM still needs to be verified with future observations; however, it provides potentially the best candidate for a DM-confined HVC.



## ACKNOWLEDGEMENTS

NM acknowledges support from the Spanish taxpayers through a Ramón y Cajal fellowship and the Consolider-Ingenio 2010 Programme under grant MultiDark CSD2009-00064. All numerical simulations were conducted on the RCC Midway cluster at the University of Chicago. OA is grateful to Doug Rudd for making the use of the Midway cluster a smooth experience. We thank Tarek Hassan for his help with general technicalities.

## REFERENCES

- Abdo A. A. et al., 2010, *ApJ*, 712, 147  
 Ackermann M. et al., 2010, *J. Cosmol. Astropart. Phys.*, 05, 025  
 Agertz O., Kravtsov A. V., Leitner S. N., Gnedin N. Y., 2013, *ApJ*, 770, 25  
 Baltz E. A. et al., 2008, *J. Cosmol. Astropart. Phys.*, 7, 13  
 Belokurov V. et al., 2007, *ApJ*, 654, 897  
 Bland-Hawthorn J., Veilleux S., Cecil G. N., Putman M. E., Gibson B. K., Maloney P. R., 1998, *MNRAS*, 299, 611  
 Blitz L., Spergel D. N., Teuben P. J., Hartmann D., Burton W. B., 1999, *ApJ*, 514, 818  
 Boothroyd A. I., Blagrove K., Lockman F. J., Martin P. G., Pinheiro Gonçalves D., Srikanth S. 2011, *A&A*, 536, A81  
 Boylan-Kolchin M., Bullock J. S., Kaplinghat M. 2012, *MNRAS*, 422, 1203  
 Bregman J. N., 1980, *ApJ*, 236, 577  
 Charbonnier A. et al., 2011, *MNRAS*, 418, 1526  
 Charbonnier A., Combet C., Maurin D., 2012, *Comput. Phys. Commun.*, 183, 656  
 Chynoweth K. M., Langston G. I., Yun M. S., Lockman F. J., Rubin K. H. R., Scoles S. A., 2008, *AJ*, 135, 1983  
 Chynoweth K. M., Langton G. I., Holley-Bockelmann K., 2011, *AJ*, 141, 9  
 CTA Consortium 2013, *Astropart. Phys.*, 43, 3  
 de Gouveia Dal Pino E. M., Melioli C., D’Ercole A., Brighenti F., Raga A. C., 2009, *Rev. Mex. Astron. Astrofis. Ser. Conf.*, 36, 17  
 Diemand J., Kuhlen M., Madau P., 2007, *ApJ*, 667, 859  
 Doró M. et al., 2013, *Astropart. Phys.*, 43, 189  
 Drlica-Wagner A., Gomez-Vargas G. A., Hewitt J. W., Linden T., Tibaldo L., 2014, preprint ([arXiv:1405.1030](https://arxiv.org/abs/1405.1030))  
 Einasto J., 1965, *Tr. Astrofizicheskogo Inst. Alma-Ata*, 51, 87  
 Ekta, Chengalur J. N., Pustilnik S. A., 2008, *MNRAS*, 391, 881  
 Ford H. A., Lockman F. J., McClure-Griffiths N. M., 2010, *ApJ*, 722, 367  
 Fornengo N., Pieri L., Scopel S., 2004, *Phys. Rev. D*, 70, 103529  
 Gaensler B. M., Madsen G. J., Chatterjee S., Mao S. A., 2008, *PASA*, 25, 184  
 Gatto A., Fraternali F., Read J. I., Marinacci F., Lux H., Walch S., 2013, *MNRAS*, 433, 2749  
 Grevech J., Putman M. E., 2009, *ApJ*, 696, 385  
 Hill A. S., Mao S. A., Benjamin R. A., Lockman F. J., McClure-Griffiths N. M., 2013, *ApJ*, 777, 55  
 Kalberla P. M. W., Dedes L., 2008, *A&A*, 487, 951  
 Klypin A., Kravtsov A. V., Valenzuela O., Prada F., 1999, *ApJ*, 522, 82  
 Konz C., Brüns C., Birk G. T., 2002, *A&A*, 391, 713  
 Lockman F. J., Benjamin R. A., Heroux A. J., Langston G. I., 2008, *ApJ*, 679, L2  
 Mateo M., 1998, *ARA&A*, 36, 435  
 Mirabal N., 2013, *MNRAS*, 432, 71  
 Moore B., Ghigna S., Governato F., Lake G., Quinn T., Stadel J., Tozzi P., 1999, *ApJ*, 524, L19  
 Moore B., Kazantzidis S., Diemand J., Stadel J., 2004, *MNRAS*, 354, 522  
 Natarajan A., Peterson J. B., Voytek T. C., Spekkens K., Mason B., Aguirre J., Willman B., 2013, *Phys. Rev. D*, 88, 083535  
 Navarro J. F., Frenk C. S., White S. D. M., 1996, *ApJ*, 462, 563  
 Navarro J. F. et al., 2010, *MNRAS*, 402, 21  
 Nichols M., Bland-Hawthorn J., 2009, *ApJ*, 707, 1642  
 Nolan P. L. et al., 2011, *ApJS*, 199, 31  
 Pidopryhora Y., Lockman F. J., Shields J. C., 2007, *ApJ*, 656, 928  
 Plöckinger S., Hensler G., 2012, *A&A*, 547, A43  
 Putman M. E., 2004, in van Woerdeneds H., Wakker B. P., Schwarz U. J., de Boer K. S., eds, *Astrophysics and Space Science Library*, Vol. 312, *High Velocity Clouds*. Kluwer, Dordrech, p. 101  
 Putman M. E., Bland-Hawthorn J., Veilleux S., Gibson B. K., Freeman K. C., Maloney P. R., 2003, *ApJ*, 597, 948  
 Putman M. E., Saul D. R., Mets E., 2011, *MNRAS*, 418, 1575  
 Putman M. E., Peek J. E. G., Joungh M. R., 2012, *ARA&A*, 50, 491  
 Quilis V., Moore B., 2001, *ApJ*, 555, L95  
 Saul D. R. et al., 2012, *ApJ*, 758, 44  
 Savage B. D., Wakker B. P., 2009, *ApJ*, 702, 1472  
 Smith G. P., 1963, *Bull. Astron. Inst. Neth.*, 17, 203  
 Springel V. et al., 2008, *MNRAS*, 391, 1685  
 Teyssier R., 2002, *A&A*, 385, 337  
 The Fermi-LAT Collaboration et al., 2014, *Phys. Rev. D*, 89, 042001  
 Thilker D. A., Braun R., Walterbos R. A. M., Corbelli E., Lockman F. J., Murphy E., Maddalena R., 2004, *ApJ*, 601, L39  
 Wakker B. P., van Woerden H., 1997, *ARA&A*, 35, 217  
 Wakker B. P., York D. G., Wilhelm R., Barentine J. C., Richter P., Beers T. C., Ivezić Ž., Howk J. C., 2008, *ApJ*, 672, 298  
 Weinberg D. H., Bullock J. S., Governato F., Kuzio de Naray R., Peter A. H. G., 2013, preprint ([arXiv:1306.0913](https://arxiv.org/abs/1306.0913))  
 Westmeier T., Brüns C., Kerp J., 2008, *MNRAS*, 390, 1691  
 Willman B. et al., 2005, *ApJ*, 626, L85  
 Wolfire M. G., McKee C. F., Hollenback D., Tielens A. G. G. M., 1995, *ApJ*, 453, 673

This paper has been typeset from a  $\text{\TeX}/\text{\LaTeX}$  file prepared by the author.